# Hybrid 3D simulations on cylinder at Re=1M

F. Miralles, S.Wornom, B.Koobus, A.Dervieux

IMAG, Université de Montpellier

13 juillet 2021

# Brief description

- RANS closure term

$$\tau^{RANS} = \left( \overbrace{0}^{\rho}, \overbrace{\mathbf{0}}^{\rho\mathbf{u}}, \overbrace{0}^{\rho E}, \overbrace{\tau : \nabla\mathbf{u} - \rho\epsilon}^{\rho k}, \overbrace{(C_1 \tau : \nabla\mathbf{u} - C_2 \rho\epsilon + E) T^{-1}}^{\rho\epsilon} \right)$$

- DDES closure term $\rho\epsilon$ is remplaced by $\rho \frac{k^{3/2}}{l_{ddes}}$ where :

$$l_{ddes} = \frac{k^{\frac{3}{2}}}{\epsilon} - f_{ddes} \max\left(0, \frac{k^{\frac{3}{2}}}{\epsilon} - 0.65\Delta_T\right), \quad \begin{aligned} f_{ddes} &= 1 - \tanh((8r_d)^3), \\ r_d &= \frac{\nu_t + \nu}{\kappa^2 y^2 \max(\sqrt{\nabla\mathbf{u} : \nabla\mathbf{u}}, 10^{-10})} \end{aligned}$$

- VMS closure term with dynamics coefficients $\mathcal{C}_s = \mathcal{C}_s(\mathbf{x}, t)$ and $Pr_t = Pr_t(\mathbf{x}, t)$

$$\tau^{DVMS}(W_h) = \left(0, \mathbf{M}_S(W_h, \phi_h^{'}), M_H(W_h, \phi_h^{'}), 0, 0\right)$$

where :

$$\begin{array}{rcl} \mathbf{M}_S(W_h, \phi_i') & = & \sum_{T\in\Omega_h} \int_T \rho_h(\mathcal{C}_s\Delta_T)^2|S'|\mathcal{D}(S')\nabla\phi_i' d\mathbf{x}, \\ M_H(W_h, \phi_i') & = & \sum_{T\in\Omega_h} \int_T \rho_h \frac{C_p(\mathcal{C}_s\Delta_T)^2}{Pr_t}|S'|\nabla T' \cdot \nabla\phi_i' d\mathbf{x} \end{array}$$

and $\phi_h^{'} = \phi_h - \overline{\phi_h}$ where $\overline{\phi_h}$ is computed from macro cells.

- Hybrid description

$$\left(\frac{\partial \overline{W}_h}{\partial t}, \chi_i\right) + \left(\nabla \cdot F(\overline{W}_h), \chi_i\right) = \theta\left(\tau^C(\overline{W}_h), \phi_i\right) + (1-\theta)\left(\tau^{DVMS}(W_h^{'}), \phi_i^{'}\right).$$

$\tau^C \in \{\tau^{RANS}, \tau^{DDES}\}$

# Hybridation function

- Definition of blending function

$$\theta = 1 - f_{ddes}$$

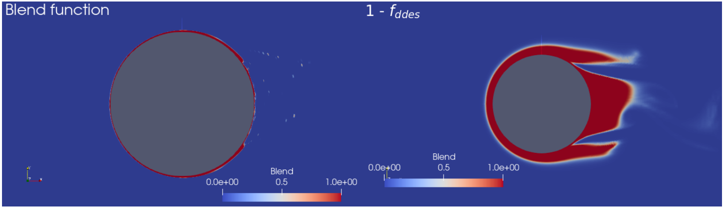


Figure – Comparaison between $\theta = 1 - f_{ddes}$ blending function, on left used for hybrid DDES and on right used for hybrid RANS.

- Zonal approach with length scale

$$\theta = \exp\left(-\frac{1}{2\epsilon_0} d(\mathbf{x}, V_{k,\epsilon})^2\right),$$

where $V_{k,\epsilon} = \{x \in \Omega_f \mid \frac{k^{3/2}(\mathbf{x})}{\epsilon(\mathbf{x})} < \Delta_{les}\}$

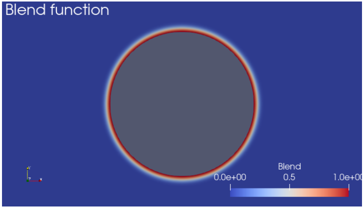


Figure – Blending surface.

- Blending function with protection zone

$$\theta = 1 - f_{ddes} \times (1 - \overline{\theta}),$$

with $\overline{\theta} = \tanh\left(\left(\frac{\Delta_T}{k^{3/2}}\epsilon\right)^2\right)$

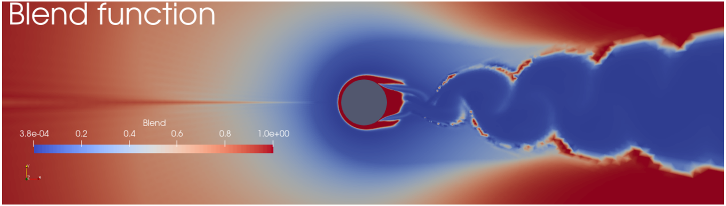


Figure – Hybrid RANS blending surface.

# Simulation with the wall law at Reynolds 1M

- Reichardt wall law :

$$U^+ = \frac{1}{\kappa}\ln\left(1+\kappa y^+\right) + 7.8\left[1 - \exp\left(\frac{-y^+}{11}\right) - \frac{-y^+}{11}\exp\left(\frac{-y^+}{3}\right)\right]$$

- Simulation set up :
  - mach number : 0.1 (subsonic flow)
  - reference pressure : 101300 $[\mathrm{N/m^2}]$
  - density : 1.22 $[\mathrm{kg/m^3}]$

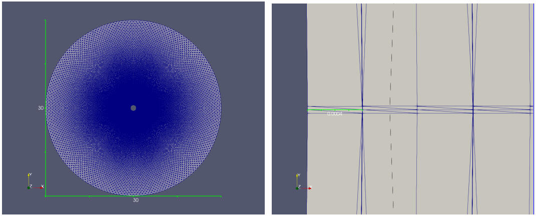


Figure – Computationnal domain on left, size of cell $h$ close to the cylinder on the rigth computed such that : $h\frac{Re}{20} = y^+ = 20 \Rightarrow h = 4.10^{-4}$.

| Name | Mesh size | $y^+$ | $\overline{C}_d$ | $C_l'$ | $-\overline{C}_{pb}$ | $\overline{L_r}$ | $\overline{\theta}$ |
|---|---|---|---|---|---|---|---|
| Present simulation | | | | | | | |
| **DDES $k-\epsilon$ Goldberg** | **4.8M** | **100** | **0.20** | **0.03** | **0.22** | **0.87** | **138** |
| DDES/ DVMS Smagorinsky | | | | | | | |
| $f = \mathbf{1} - \tanh((\mathbf{8}r_d)^{\mathbf{3}})$ **et** $\overline{\theta} = \tanh(\left(\frac{\Delta_T}{k^{3/2}}\epsilon\right)^{\mathbf{2}})$ | **4.8M** | **100** | **0.20** | **0.016** | **0.22** | **0.82** | **135** |
| $f = \mathbf{1} - \tanh((\mathbf{8}r_d)^{\mathbf{3}})$ **et** $\overline{\theta} = \tanh(\left(\frac{\Delta_T}{k^{3/2}}\epsilon\right)^{\mathbf{2}})$ | **4.8M** | **200** | **0.13** | **0.015** | **0.05** | **0.82** | **135** |
| $\theta = \exp(-\frac{\mathbf{1}}{\mathbf{2}\epsilon}d(r, V)^{\mathbf{2}})$ | **4.8M** | **100** | **0.20** | **0.005** | **0.24** | **0.92** | **132** |
| $\theta = \exp(-\frac{\mathbf{1}}{\mathbf{2}\epsilon}d(r, V)^{\mathbf{2}})$ | **4.8M** | **200** | **0.14** | **0.001** | **0.05** | **0.58** | **144** |
| $\theta = \mathbf{1} - \tanh((\mathbf{8}r_d)^{\mathbf{3}})$ | **4.8M** | **100** | **0.20** | **0.01** | **0.21** | **0.82** | **133** |
| $\theta = \mathbf{1} - \tanh((\mathbf{8}r_d)^{\mathbf{3}})$ | **4.8M** | **200** | **0.14** | **0.01** | **0.04** | **0.58** | **142** |
| Other simulations | | | | | | | |
| **Catalano [1]** | **2.3M** | **-** | **0.31-0.40** | **-** | **0.32-0.41** | | |
| **LES Kim [3]** | **6.8M** | **-** | **0.27** | **0.12** | **0.28** | **-** | **108** |
| Expériences | | | | | | | |
| **Gölling [9]** | | | | | | **-** | **130** |
| **Zdravkovich [8]** | | | **0.2-0.4** | **0.1-0.15** | **0.2-0.34** | | |

Table – Bulk coefficient of the flow around a circular cylinder at Reynolds number 1M, $\overline{C}_d$ holds for the mean drag coefficient, $C_l'$ is the root mean square of lift time fluctuation, $\overline{C}_{p_b}$ is the pressure coefficient at cylinder basis, $\overline{L_r}$ is the mean recirculation lenght, $\overline{\theta}$ is the mean separation angle.

| Name | Mesh size | $y^+$ | $\overline{C}_d$ | $C'_l$ | $-\overline{C}_{pb}$ | $\overline{L_r}$ | $\overline{\theta}$ |
|---|---|---|---|---|---|---|---|
| Present simulation | | | | | | | |
| **DDES $k-\epsilon$ Goldberg** | **4.8M** | **100** | **0.20** | **0.03** | **0.22** | **0.87** | **138** |
| DDES/ DVMS Smagorinsky | | | | | | | |
| $f = \mathbf{1} - \tanh((\mathbf{8}r_d)^{\mathbf{3}})$ **et** $\overline{\theta} = \tanh(\left(\frac{\Delta_T}{k^{3/2}}\epsilon\right)^{2})$ | **4.8M** | **100** | **0.20** | **0.016** | **0.22** | **0.82** | **135** |
| $f = \mathbf{1} - \tanh((\mathbf{8}r_d)^{\mathbf{3}})$ **et** $\overline{\theta} = \tanh(\left(\frac{\Delta_T}{k^{3/2}}\epsilon\right)^{2})$ | **4.8M** | **200** | **0.13** | **0.015** | **0.05** | **0.82** | **135** |
| $\theta = \exp(-\frac{1}{2\epsilon}d(r,V)^{2})$ | **4.8M** | **100** | **0.20** | **0.005** | **0.24** | **0.92** | **132** |
| $\theta = \exp(-\frac{1}{2\epsilon}d(r,V)^{2})$ | **4.8M** | **200** | **0.14** | **0.001** | **0.05** | **0.58** | **144** |
| $\theta = \mathbf{1} - \tanh((\mathbf{8}r_d)^{\mathbf{3}})$ | **4.8M** | **100** | **0.20** | **0.01** | **0.21** | **0.82** | **133** |
| $\theta = \mathbf{1} - \tanh((\mathbf{8}r_d)^{\mathbf{3}})$ | **4.8M** | **200** | **0.14** | **0.01** | **0.04** | **0.58** | **142** |
| RANS / DVMS Smagorinsky | | | | | | | |
| $f = \mathbf{1} - \tanh((\mathbf{8}r_d)^{\mathbf{3}})$ **et** $\overline{\theta} = \tanh(\left(\frac{\Delta_T}{k^{3/2}}\epsilon\right)^{2})$ | **4.8M** | **100** | **0.24** | **0.05** | **0.22** | **0.62** | **133** |
| $f = \mathbf{1} - \tanh((\mathbf{20}r_d)^{\mathbf{3}})$ **et** $\overline{\theta} = \tanh((\mathbf{20}r_d)^{\mathbf{3}})$ | **4.8M** | **100** | **0.24** | **0.06** | **0.23** | **0.58** | **133** |
| $f = \mathbf{1} - \tanh((\mathbf{8}r_d)^{\mathbf{3}})$ **et** $\overline{\theta} = \tanh((\mathbf{8}r_d)^{\mathbf{3}})$ | **4.8M** | **100** | **0.24** | **0.06** | **0.21** | **0.60** | **134** |
| $\theta = \exp(-\frac{1}{2\epsilon}d(r,V)^{2})$ | **4.8M** | **100** | **0.20** | **0.02** | **0.17** | **0.78** | **134** |
| $\theta = \mathbf{1} - \tanh((\mathbf{8}r_d)^{\mathbf{3}})$ | **4.8M** | **100** | **0.25** | **0.06** | **0.19** | **0.72** | **133** |
| Other simulations | | | | | | | |
| **Catalano [1]** | **2.3M** | **-** | **0.31-0.40** | **-** | **0.32-0.41** | | |
| **LES Kim [3]** | **6.8M** | **-** | **0.27** | **0.12** | **0.28** | **-** | **108** |
| Expériences | | | | | | | |
| **Gölling [9]** | | | | | | **-** | **130** |
| **Zdravkovich [8]** | | | **0.2-0.4** | **0.1-0.15** | **0.2-0.34** | | |

Table – Bulk coefficient of the flow around a circular cylinder at Reynolds number 1M, $\overline{C}_d$ holds for the mean drag coefficient, $C'_l$ is the root mean square of lift time fluctuation, $\overline{C}_{p_b}$ is the pressure coefficient at cylinder basis, $\overline{L_r}$ is the mean recirculation lenght, $\overline{\theta}$ is the mean separation angle.

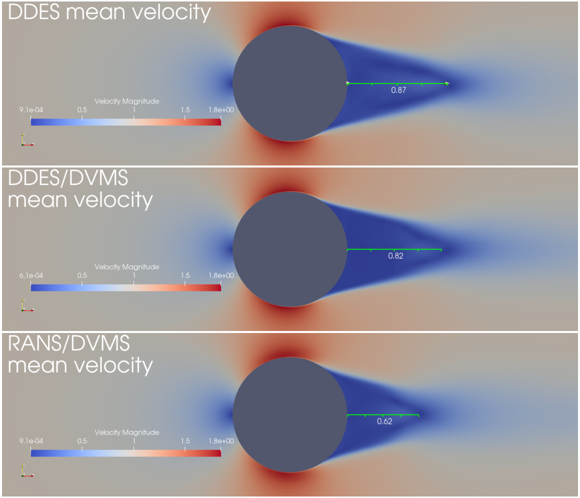


Figure – Recirculation zone comparaison between hybrid models (WL case).

■ Result summary and comparaison with ITW

| Name | Mesh size | $y^+$ | $\overline{C}_d$ | $C_l'$ | $-\overline{C}_{pb}$ | $\overline{L_r}$ | $\overline{\theta}$ |
|---|---|---|---|---|---|---|---|
| Present simulation | | | | | | | |
| DDES $k-\epsilon$ Goldberg WL | 4.8M | 100 | 0.20 | 0.03 | 0.22 | 0.87 | 138 |
| DDES $k-\epsilon$ Goldberg ITW | 4.8M | 100 | 0.50 | 0.06 | 0.54 | 1.22 | 103 |
| DDES/ DVMS Smagorinsky WL | 4.8M | 100 | 0.20 | 0.016 | 0.22 | 0.82 | 135 |
| DDES/ DVMS Smagorinsky ITW | 4.8M | 100 | 0.51 | 0.07 | 0.28 | 0.85 | 110 |
| RANS / DVMS Smagorinsky WL | 4.8M | 100 | 0.24 | 0.05 | 0.22 | 0.62 | 133 |
| RANS / DVMS Smagorinsky ITW | 4.8M | 100 | 0.47 | 0.08 | 0.34 | 0.62 | 110 |
| Other simulations | | | | | | | |
| Catalano [1] | 2.3M | - | 0.31-0.40 | - | 0.32-0.41 | | |
| LES Kim [3] | 6.8M | - | 0.27 | 0.12 | 0.28 | - | 108 |
| Expériences | | | | | | | |
| Gölling [9] | | | | | | - | 130 |
| Zdravkovich [8] | | | 0.2-0.4 | 0.1-0.15 | 0.2-0.34 | | |

Table – Bulk coefficient of the flow around a circular cylinder at Reynolds number 1M, $\overline{C}_d$ holds for the mean drag coefficient, $C_l'$ is the root mean square of lift time fluctuation, $\overline{C}_{p_b}$ is the pressure coefficient at cylinder basis, $\overline{L_r}$ is the mean recirculation lenght, $\overline{\theta}$ is the mean separation angle.

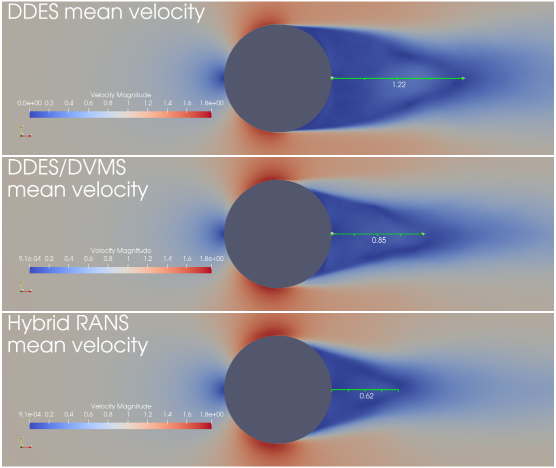


Figure – Recirculation zone comparaison between hybrid models (ITW case ).

- Pressure coefficient

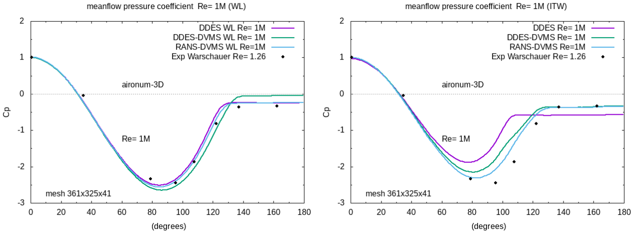


Figure – Distribution of mean pressure as a function of polar angle. Comparaison between experiment. Wall law on the left and integration to the wall on the right.

## Velocity profile

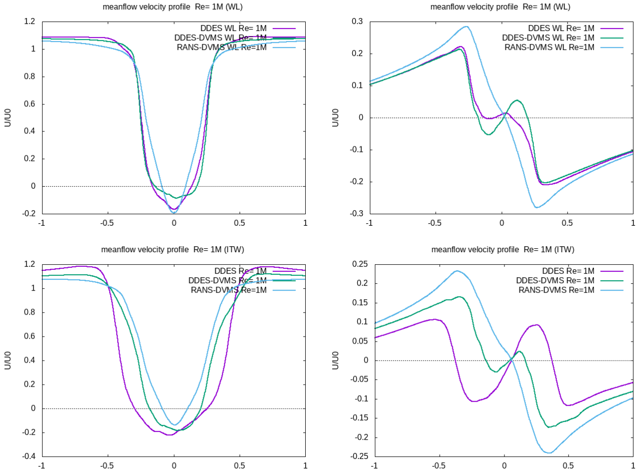


Figure – On the top longitudonal velocity profile at $x/D = 1$, and on bottom the transverse velocity.

## Wall Law Q-criteria

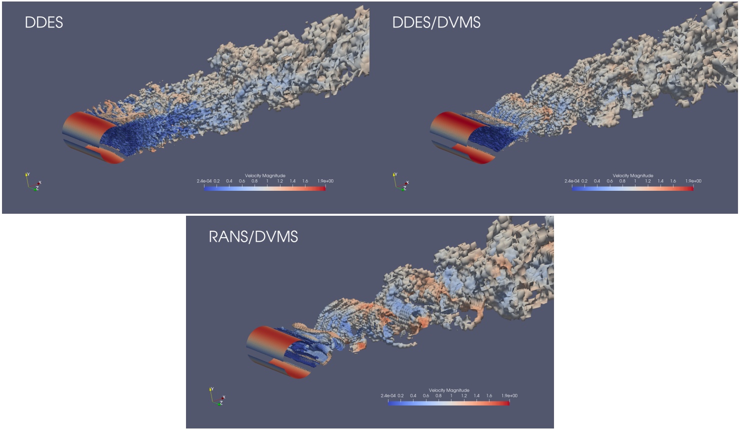


Figure – Q-critera contour using velocity color scale.

- Integration to the Wall Q-criteria

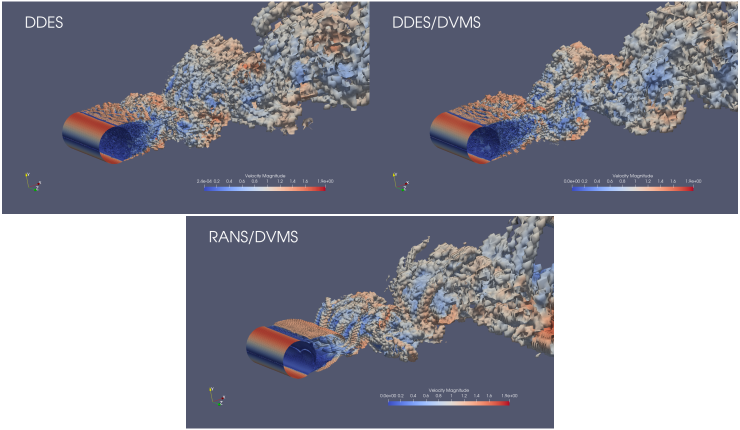


Figure – Q-critera contour using velocity color scale.

## Conclusions and things to do

- Hybrid function with protection zone give better results,
- surface pressure coefficient is close to experimental data for WL,
- Bulks coefficients are good with RANS/DVMS model,
- Improve blend function to catch eddies at starting region of the wake,
- Test influence of WALE SGS model.

- P. Catalano, M.Wang, G. Iaccarino and P. Moin. Numerical simulation of the flow around a circular cylinder at High Reynolds numbers. *International Journal of Heat and Fluid Flow*, 24 :463-469, 2003.
- Y. Ono and T. Tamura. LES of flows around a circular cylinder in the critical Reynolds number region. *Proceedings of BBAA VI International Colloquium on : Bluff Bodies Aerodynamics and Applications*, Milano, Italy, July 20-24 2008.
- S.E. Kim and L.S. Mohan. Prediction of unsteady loading on a circular cylinder in high Reynolds number flows using large eddy simulation. *Proceedings of OMAE 2005 : 24th International Conference on Offshore Mechanics and Artic Engin.*
- G. Schewe. On the force fluctuations acting on a circular cylinder in crossflow from subcritical up to transcritical Reynolds numbers. *Journal of Fluid Mechanics*, 133 :265-285, 1983.
- W.C. L. Shih, C.Wang, D. Coles and A. Roshko. Experiments on Flow past rough circular cylinders at large Reynolds numbers. *Journal of Wind Engeneering and Industrial Aerodynamics*, 49 :351-368, 1993.
- E. Szechenyi. Supercritical reynolds number simulation for two-dimensional flow over circular cylinders. *Journal of Fluid Mechanics*, 70 :529-542, 1975.
- O. Guven, C. Farell, and V.C. Patel. Surface-roughness effects on the mean flow past circular cylinders. *Journal of Fluid Mechanics*, 98(4) :673-701, 1980.
- M.M. Zdravkovich. Flow around circular cylinders Vol 1 : Fundamentals. *Oxford University Press*, 1997.
- B. Gölling. Experimental Investigations of Separating Boundary-Layer Flow from Circular Cylinder at Reynolds Numbers from 105 up to 107 ; three-dimensional vortex flow of a circular cylinder. *G.E.A. Meier and K.R. Sreenivasan, editors, Proceedings of IUTAM Symposium on One Hundred Years of Boundary Layer Research*, pages 455-462, The Netherlands, 2006. Springer.